Dalton Transactions



PAPER View Journal | View Issue



Cite this: *Dalton Trans.*, 2022, **51**, 17629

biological activity†

Ariadni Zianna, *\bar{\mathbb{0}} *\alpha^a Ellie Vradi, *\bar{\mathbb{0}} Antonios G. Hatzidimitriou, *\alpha Stavros Kalogiannis *\bar{\mathbb{0}} and George Psomas *\bar{\mathbb{0}} *\alpha^a

Zinc(II) complexes of 3-bromo-5-chloro-

salicylaldehyde: characterization and

Five neutral zinc(II) complexes of 3-bromo-5-chloro-salicylaldehyde (3-Br-5-Cl-saloH) were synthesized in the absence or presence of the nitrogen-donor co-ligands 2,2'-bipyridine (bipy), 1,10-phenanthroline (phen), 2,9-dimethyl-1,10-phenanthroline (neoc), or 2,2'-bipyridylamine (bipyam) and were characterized by various techniques. The obtained complexes were $[Zn(3-Br-5-Cl-salo)_2(H_2O)_2]$ (1), $[Zn(3-Br-5-Cl-salo)_2(bipy)]$ (2), $[Zn(3-Br-5-Cl-salo)_2(phen)]$ (3), $[Zn(3-Br-5-Cl-salo)_2(neoc)]$ (4) and $[Zn(3-Br-5-Cl-salo)_2(bi-pyam)]$ (5). The crystal structures of complexes 1 and 3 were determined by single-crystal X-ray crystallography. The interaction of the compounds with calf-thymus DNA takes place *via* intercalation. The compounds may moderately cleave pBR322 plasmid DNA at a concentration of 500 μ M. The compounds may bind tightly and reversibly to serum albumins. The antioxidant activity of the compounds was examined towards 1,1-diphenyl-picrylhydrazyl and 2,2'-azinobis(3-ethylbenzothiazoline-6-sulfonic acid) radicals and H_2O_2 . The antimicrobial potency of the compounds was investigated against *Staphylococcus aureus* ATCC 6538, *Bacillus subtilis* ATCC 6633, *Escherichia coli* NCTC 29212 and *Xanthomonas campestris* ATCC 1395.

Received 24th July 2022, Accepted 31st October 2022 DOI: 10.1039/d2dt02404g

rsc.li/dalton

1. Introduction

In recent years, there has been increasing interest in the design of new complexes suitable as drug candidates. In the human body, a drug interacts with DNA, which is a storage and carrier molecule of genetic information, RNA and proteins. ¹⁻⁴ Until recently, most compounds used as medicines were almost exclusively purely organic. At the beginning of the 20th century, the first arsenic organometallic complex for the treatment of syphilis (salvarsan) was applied. Since then, many other metal complexes were discovered, such as the Au complex agent Auranofin and the Pt-based anticancer drugs cisplatin, oxaliplatin and carboplatin. Despite their high activity in such diseases, little attention has been paid to their application as antimicrobial compounds. ⁵

Salicylaldehyde is a natural product with oily pale-yellow color and bitter almond odor and is an ingredient of a defensive secretion of some leaf beetle species. A number of substituted salicylaldehydes have been found to present significant antimicrobial properties against bacteria and yeasts, while some complexes could be used as potential therapeutic agents against *Candida* infections. In order to present high antimicrobial activity, substituents on the benzene ring are required, and halogenation often gives highly active compounds; however, their antimicrobial potency is not easily predictable and the mechanism of action of these agents still remains unknown. One possibility is that their antimicrobial activity is due to the formation of Schiff bases with amino groups of the microbial cells. ⁷⁻⁹

Coordination of salicylaldehydes to metal ions may enhance their antimicrobial properties. $^{1,10-12}$ Apart from their antimicrobial properties, salicylaldehydes and their metal complexes have the ability to interact with important biomolecules, such as DNA and RNA. For example, mixed-ligand Cu(II) complexes of 5-nitro-salicylaldehyde and 2-hydroxynaphthaldehyde act as artificial nucleases, 1 a Cu(II) complex with 2-hydroxynaphthaldehyde presented interesting results regarding its DNA/RNA binding, cleavage and cytotoxicity 13 and a series of mixed-ligand Cu(II) complexes of substituted salicylaldehydes and α -diimines exhibited antiproliferative properties. 14

^aLaboratory of Inorganic Chemistry, Department of Chemistry, Aristotle University of Thessaloniki, GR-54124 Thessaloniki, Greece. E-mail: ariadnezianna@gmail.com, gepsomas@chem.auth.gr

^bDepartment of Nutritional Sciences and Dietetics, International Hellenic University, Sindos, GR-57400 Thessaloniki, Greece

[†]Electronic supplementary information (ESI) available. CCDC 2191080 and 2191081. For ESI and crystallographic data in CIF or other electronic format see DOI: https://doi.org/10.1039/d2dt02404g

Among the plethora of metal ions, zinc is the second most common trace element in the human body and it is vital to the structure and function of circa 2800 macromolecules and 300 enzymes and is a component of 10% of human proteins. Zinc metallothioneins are metal-binding proteins that present high affinity to divalent trace metals. Metallothioneins can scavenge hydroxyl radicals 300 times higher than glutathione, so they protect biological structures and DNA from oxidative damage. Zinc is also a co-factor of the cytosolic and extracellular Zn/Cu SOD enzyme, which acts as an ROS scavenger by catalyzing the dismutation of O₂ radicals into the less harmful O₂ and H₂O₂. Zinc also plays an important role in innate and adaptive immunity and is very important for maintaining the membrane barrier structure and function. 15 Furthermore, zinc complexes with biological activity are found in the literature. Zinc oxide and baby zinc are used for skin injuries and infections, and deadly diarrhea in Asian and African countries, respectively. 16 Other zinc complexes have anticancer, 17 antidiabetic, 18 anticonvulsant, 19 anti-inflammatory, 20 antimicrobial 21 and antioxidant²² properties.

Our research is focused on the synthesis, characterization and investigation of the biological profile of metal complexes with substituted salicylaldehydes. Our previous works concerned metal complexes of mono- (X-salo) and bis-substituted $(3,5\text{-diX-salo})_2$ salicylaldehydes. ^{23–28} Continuing the search in this field, we have chosen 3-bromo-5-chloro-salicylaldehyde (3-Br-5-Cl-saloH, Fig. 1(A)), a ligand with two different substituents on the benzene ring (3-bromo and 5-chloro). A thorough search in the literature may reveal the existence of a copper(π) and two cobalt(π) complexes ^{29,30} with 3-bromo-5-chloro-salicylaldehyde.

We have synthesized five novel Zn(II) complexes of 3-Br-5-Cl-saloH in the absence or presence of the α -diimines 2,2'-bipyridine (bipy), 1,10-phenanthroline (phen), 2,9-dimethyl-1,10-phenanthroline (neoc), or 2,2'-bipyridylamine (bipyam)

(Fig. 1), formulated as [Zn(3-Br-5-Cl-salo)₂(H₂O)₂] (1), [Zn(3-Br-5-Cl-salo)₂(bipy)] (2), [Zn(3-Br-5-Cl-salo)₂(phen)] (3), [Zn(3-Br-5-Cl-salo)₂(neoc)] (4) and [Zn(3-Br-5-Cl-salo)₂(bipyam)]. All complexes were characterized by physicochemical and spectroscopic (IR, UV–vis and ¹H NMR) techniques and the crystal structures of complexes 1 and 3 were determined by single-crystal X-ray crystallography.

The interaction of the compounds with calf-thymus (CT) DNA was investigated by UV-vis spectroscopy, by viscosity measurements, and via their ability to displace ethidium bromide (EB) from the DNA-EB conjugate. The potential nuclease-like activity of the compounds was evaluated via the cleavage of supercoiled circular pBR322 plasmid DNA (pDNA) examined by agarose gel electrophoresis. The in vitro affinity of the complexes to bind to human serum albumin (HSA) and bovine serum albumin (BSA) was evaluated by fluorescence emission spectroscopy and the corresponding binding constants were determined. The antimicrobial activity of the compounds was examined against two Gram-positive microorganisms (Staphylococcus aureus ATCC 6538 (S. aureus) and Bacillus subtilis ATCC 6633 (B. subtilis)) and two Gram-negative microorganisms (Escherichia coli NCTC 29212 (E. coli) and Xanthomonas campestris ATCC 1395 (X. campestris)), and the minimum inhibitory concentration (MIC) was determined. The potential antioxidant activity of the compounds was evaluated by determining their ability to scavenge 1,1-diphenylpicrylhydrazyl (DPPH) and 2,2'-azinobis(3-ethylbenzothiazoline-6-sulfonic acid) (ABTS) free radicals and to reduce H₂O₂.

2 Experimental

2.1 Materials - instrumentation - physical measurements

All chemicals and solvents were reagent grade and were used as purchased from commercial sources: 3-Br-5-Cl-saloH, bipy,

CI
$$\frac{5}{4}$$
 $\frac{6}{3}$ $\frac{1}{2}$ $\frac{7}{0}$ $\frac{5}{3}$ $\frac{6}{3}$ $\frac{5}{4}$ $\frac{5}{3}$ $\frac{6}{1}$ $\frac{5}{4}$ $\frac{7}{1}$ \frac

Fig. 1 Syntax formula of (A) 3-Br-5-Cl-salicylaldehyde (3-Br-5-Cl-saloH), (B) 2,2'-bipyridine (bipy), (C) 2,2'-bipyridylamine (bipyam), (D) 1,10-phenanthroline (phen) and (E) 2,9-dimethyl-1,10-phenanthroline (neoc) with H atom labeling.

phen, neoc, bipyam, Zn(NO₃)₂·4H₂O, CH₃ONa, trisodium citrate, NaCl, BSA, HSA, CT DNA, EB, ABTS, K₂S₂O₈, NaH₂PO₄, nordihydroguaiaretic acid (NDGA) and butylated hydroxytoluene (BHT) were purchased from Sigma-Aldrich Co.; 6-hydroxy-2,5,7,8-tetramethylchromane-2-carboxylic acid (Trolox) was purchased from J&K; DPPH was bought from TCI; L-ascorbic acid and all solvents were purchased from Chemlab.

Dalton Transactions

Infrared (IR) spectra (400-4000 cm⁻¹) were recorded on a Nicolet FT-IR 6700 spectrometer with samples prepared as KBr pellets (abbreviations used: s = strong, m = medium, sm = strong-medium, w = weak). UV-visible (UV-vis) spectra were recorded as nujol mulls and in DMSO solutions at concentrations in the range 10^{-4} - 5×10^{-3} M on a Hitachi U-2001 dual-beam spectrophotometer. C, H and N elemental analyses were performed on a PerkinElmer 240B elemental microanalyzer. Molecular conductivity measurements of 1 mM DMSO solution of the complexes were carried out with a Crison Basic 30 conductometer. Fluorescence spectra were recorded in solution on a Hitachi F-7000 fluorescence spectrophotometer. Viscosity experiments were carried out using an ALPHA L Fungilab rotational viscometer equipped with an 18 mL LCP spindle and the measurements were performed at 100 rpm. ¹H NMR spectra were recorded on an Agilent 500/54 (500 MHz for ¹H) spectrometer using DMSO-d₆ as a solvent (abbreviations used: s = singlet, d = doublet, dd = double-doublet, br = broad, m = multiplet).

DNA stock solution was prepared by dilution of CT DNA with buffer (containing 150 mM NaCl and 15 mM trisodium citrate at pH 7.0) followed by stirring for 1 h, and kept at 4 °C for no longer than a week. The stock solution of CT DNA gave a ratio of UV absorbance at 260 and 280 nm (A_{260}/A_{280}) of ~1.88, indicating that the DNA was sufficiently free of protein contamination.³¹ The DNA concentration per nucleotide was determined by UV absorbance at 260 nm after 1:20 dilution using ε = 6600 M⁻¹ cm⁻¹.³²

2.2 Synthesis of the complexes

Complexes 1–5 were synthesized according to the published procedure. Complex 1 was prepared by the addition of a methanolic solution of 3-Br-5-Cl-saloH (1 mmol, 235 mg) deprotonated by CH₃ONa (1 mmol, 54 mg) to a methanolic solution of $Zn(NO_3)_2\cdot 4H_2O$ (0.5 mmol, 130 mg) at room temperature. The reaction mixture was stirred for 1 h, filtered and left for slow evaporation at room temperature. For the mixed-ligand complexes 2–5, a methanolic solution of the corresponding α -diimine (0.5 mmol) was added to the above mixture and the reaction mixture was stirred further for 1 h, filtered and left for slow evaporation at room temperature. After a few days, yellow single-crystals of complexes 1 and 3 suitable for X-ray structure determination were collected and air-dried.

2.2.1 [Zn(3-Br-5-Cl-salo)₂(H₂O)₂] (1). Yellow crystalline product (yield: 182 mg, 65%), analyzed as [Zn(3-Br-5-Cl-salo)₂(H₂O)₂], (C₁₄H₁₀Br₂Cl₂O₆Zn) (MW = 570.33): C: 24.48, H: 1.77%; found: C: 24.55, H: 1.85%. IR (KBr): selected peaks (cm⁻¹): 3390(m), ν (O-H)_{coordinated water}; 1641(s), ν (C=O); 1308(m), ν (C-O \rightarrow Zn). UV-vis: as nujol mulls, λ (nm): 339,

421; in DMSO, λ (nm) (ε , M⁻¹ cm⁻¹): 338 (2600), 423 (6800). ¹H NMR (DMSO-d₆), δ (ppm): 9.45 (2H, s, H⁷ 3-Br-5-Cl-salo), 7.71 (2H, d, H⁶ 3-Br-5-Cl-salo), 7.52 (2H, dd, H⁴ 3-Br-5-Cl-salo). $\Lambda_{\rm M}$ (in 1 mM DMSO solution) = 6 mho cm² mol⁻¹.

2.2.2 [Zn(3-Br-5-Cl-salo)₂(bipy)] (2). Yellow microcrystalline product (yield: 222 mg, 64%), analyzed as [Zn(3-Br-5-Cl-salo)₂ (bipy)], (C₂₄H₁₄Br₂Cl₂N₂O₄Zn) (MW = 690.49): C: 41.74, H: 2.04, N: 4.06%; found: C: 41.65, H: 2.11, N: 4.18%. IR (KBr), selected peaks (cm⁻¹): 1628(s) ν (C=O), 1318(m) ν (C-O \rightarrow Zn), 767(m) ρ (C-H)_{bipy}; UV-vis: as nujol mulls, λ (nm): 310(sh), 422; in DMSO, λ (nm) (ε , M⁻¹ cm⁻¹): 309 (sh), 422 (5500). ¹H NMR (DMSO-d₆), δ (ppm): 9.55 (2H, s, H⁷ 3-Br-5-Cl-salo), 8.72 (2H, H³- and H^{3'}-bipy), 8.62 (2H, br, H⁴- and H^{4'}-bipy), 8.25 (2H, m, H⁵- and H^{5'}-bipy), 7.74 (2H, d, H⁶- and H^{6'}-bipy), 7.62 (2H, d, H⁶ 3-Br-5-Cl-salo), 7.38 (2H, dd, H⁴ 3-Br-5-Cl-salo). Λ _M (in 1 mM DMSO solution) = 12 mho cm² mol⁻¹.

2.2.3 [Zn(3-Br-5-Cl-salo)₂(phen)] (3). Yellow single-crystals suitable for X-ray determination (180 mg, yield 50%), analyzed as [Zn(3-Br-5-Cl-salo)₂(phen)] ($C_{26}H_{14}Br_2Cl_2N_2O_4Zn$) (M.W. = 714.51) C: 43.71, H: 1.97, N: 3.92%; found: C: 43.79, H: 2.05, N: 4.07%. IR (KBr), selected peaks (cm⁻¹): 1625(s), ν (C=O); 1318(m), ν (C-O \rightarrow Zn); 724(m), ρ (C-H)_{phen}. UV-vis: as nujol mulls, λ (nm): 325 (sh), 422; in DMSO, λ (nm) (ε , M⁻¹ cm⁻¹): 425 (5000). ¹H NMR (DMSO-d₆), δ (ppm): 9.58 (2H, s, H⁷ 3-Br-5-Cl-salo), 9.04 (2H, br, H²- and H⁹-phen), 8.91 (2H, H⁴- and H⁷-phen), 8.28 (2H, s, H⁵- and H⁶-phen), 8.11 (2H, m, H³- and H⁸-phen), 7.61 (2H, br, H⁶ 3-Br-5-Cl-salo), 7.34 (2H, m, H⁴ 3-Br-5-Cl-salo). $\Lambda_{\rm M}$ (in 1 mM DMSO solution) = 15 mho cm² mol⁻¹.

2.2.4 [Zn(3-Br-5-Cl-salo)₂(neoc)] (4). Yellow microcrystalline product (218 mg, yield 59%) analyzed as [Zn(3-Br-5-Cl-salo)₂ (neoc)], (C₂₈H₁₈Br₂Cl₂N₂O₄Zn) (MW = 742.57) C: 45.29, H: 2.44, N: 3.77%; found: C: 45.35, H: 2.52, N: 3.85%. IR (KBr), selected peaks (cm⁻¹): 1641(s), ν (C=O); 1324(m), ν (C-O \rightarrow Zn), 729 (sm), ρ (C-H)_{neoc}. UV-vis: as nujol mulls, λ (nm): 329(sh), 418; in DMSO, λ (nm) (ε , M⁻¹ cm⁻¹): 329 (sh), 418 (11400). ¹H NMR (DMSO-d₆), δ (ppm): 9.46 (2H, s, H⁷ 3-Br-5-Cl-salo), 8.77 (2H, d, H⁴- and H⁷-neoc), 8.32 (2H, s, H⁵- and H⁶-neoc), 7.68 (2H, br, H³- and H⁸-neoc), 7.60 (2H, br, H⁶ 3-Br-5-Cl-salo), 7.44 (2H, br, H⁴ 3-Br-5-Cl-salo), 3.00 (6H, CH₃-neoc). $\Lambda_{\rm M}$ (in 1 mM DMSO solution) = 10 mho cm² mol⁻¹.

2.2.5 [Zn(3-Br-5-Cl-salo)₂(bipyam)] (5). Yellow microcrystal-line product (208 mg, yield 59%) analyzed as [Zn(3-Br-5-Cl-salo)₂(bipyam)] ($C_{24}H_{15}Br_2C_{12}N_3O_4Zn$) (MW = 705.51) C: 40.86, H: 2.14, N: 5.96%; found: C: 40.95, H: 2.25, N: 5.75%. IR (KBr), selected peaks (cm⁻¹): 3328(w), 3205(w) and 3113(w), ν (N-H)_{bipyam}; 1654(s), δ (N-H)_{bipyam}; 1628(s), ν (C=O); 1596(s), ν (C=N); 1315(s), ν (C-O \rightarrow Zn); 767(m), ρ (C-H)_{bipyam}. UV-vis: as nujol mulls, δ (nm): 309 (sh), 335, 424; in DMSO, δ (nm) (ϵ , M⁻¹ cm⁻¹): 309 (sh), 337 (7000), 425 (1250). ¹H NMR (DMSO-d₆), δ (ppm): 9.98 (1H, br s, N-H bipyam), 9.55 (2H, s, H⁷ 3,5-diBr-salo), 8.35 (2H, d, H³- and H^{3'}-bipyam), 7.74 (4H, m, H⁵-, H^{5'}-, H⁶- and H^{6'}-bipyam), 7.62 (2H, d, H⁶ 3-Br-5-Cl-salo), 7.51 (2H, dd, H⁴ 3-Br-5-Cl-salo), 6.96 (2H, br m, H⁴- and H^{4'}-bipyam). δ _M (in 1 mM DMSO solution) = 10 mho cm² mol⁻¹.

2.3 X-ray crystal structure determination

Paper

Single-crystals of complexes 1 and 3 suitable for crystal structure analysis were obtained by slow evaporation of their mother liquids at RT. They were mounted at room temperature on a Bruker Kappa APEX2 diffractometer equipped with a Triumph monochromator using Mo Kα radiation. Unit cell dimensions were determined and refined from the angular settings of at least 163 high intensity reflections in the range $10 < \theta < 20^{\circ}$. Intensity data were recorded using φ and ω scans. Both crystals presented no decay during the data collection. The frames collected for each crystal were integrated with the Bruker SAINT Software package,33 using a narrowframe algorithm. Data were corrected for absorption using a numerical method (SADABS) based on crystal dimensions.³⁴ The structures were solved using the SUPERFLIP package, 35 incorporated in Crystals. Data refinement (full-matrix leastsquares methods on F^2) and all subsequent calculations were carried out using the Crystals version 14.61 build 6236 program package.36 All non-hydrogen atoms were refined anisotropically. Hydrogen atoms were located by difference maps at their expected positions and refined using soft constraints. By the end of the refinement, they were positioned geometrically using riding constraints to bonded Crystallographic data for complexes 1 and 3 are presented in Table S1.†

2.4 Study of the biological profile of the compounds

The biological activity (interaction with DNA and albumins and antioxidant and antimicrobial activities) of the compounds was evaluated *in vitro* after the compounds were dissolved in DMSO (1 mM), due to their low solubility in water. The studies were conducted in the presence of aqueous buffer solutions, where mixing of each solution never exceeded 5% DMSO (v/v) in the final solution. Control experiments were undertaken to assess the effect of DMSO on the data. Minimum or no changes were observed in the spectra of the SAs or CT DNA and appropriate corrections were performed, when needed.

The interaction of the compounds with CT DNA was examined thoroughly by UV-vis spectroscopy and viscosity measurements, and via competitive studies with EB by fluorescence emission spectroscopy. The ability of the compounds to cleave pBR322 plasmid DNA was studied by agarose gel electrophoresis. The serum albumin-(BSA or HSA)-binding was studied through tryptophan fluorescence quenching experiments. The antioxidant activity of the compounds was evaluated by determining their ability to scavenge the ABTS and DPPH radicals and to reduce H₂O₂. Each experiment was performed in triplicate and the standard deviation of absorbance was <10% of the mean. The antimicrobial activity of the compounds was evaluated by MIC values towards two Gram-(-) and two Gram-(+) bacterial species. All the specific protocols and relevant equations involved in the in vitro study of the biological activity of the compounds are presented in the ESI (sections S1–S5†).

3 Results and discussion

3.1 Synthesis, general aspects and characterization of the complexes

Complex 1 was prepared in methanol from the 1:2 ratio reaction of $Zn(NO_3)_2 \cdot 4H_2O$ with 3-Br-5-Cl-salo (deprotonated by CH_3ONa) according to a previously published procedure. Furthermore, the reaction of methanolic solutions of $Zn(NO_3)_2 \cdot 4H_2O$ with 3-Br-5-Cl-salo in the presence of the α -diimines bipy, phen, neoc or bipyam in a 1:2:1 (Zn^{2+}) : (3-Br-5-Cl-salo): $(\alpha$ -diimine) ratio led to the formation of complexes 2–5.

All complexes were found soluble in DMF and DMSO but insoluble in most organic solvents, H_2O and Et_2O . They are non-electrolytes in DMSO solution, since the values of the Λ_M of the complexes in 1 mM DMSO solution were found in the range 6–15 mho cm² mol⁻¹,³⁷ and elemental analysis data showed a 1:2 Zn(II): (3-Br-5-Cl-salo⁻) composition. The crystal structures of complexes 1 and 3 were further determined by single-crystal X-ray diffraction analysis.

The findings of the IR spectroscopy confirmed the deprotonation and suggested the bidentate binding mode of the 3-Br-5-Cl-salo ligand and the co-existence of the α-diimines. Free 3-Br-5-Cl-saloH presents in the IR spectrum two peaks attributed to the stretching and bending vibrations of the phenolic OH, at \sim 3200 cm⁻¹ and 1400 cm⁻¹, respectively. In the IR spectra of complexes 1-5, these two peaks disappear, due to the deprotonation and the coordination of the phenolato group of the ligand to the Zn ion. The peak of the aldehyde bond $\nu(HC=0)$ at ~1653 cm⁻¹ of free 3-Br-5-Cl-saloH is shifted towards 1625–1640 cm⁻¹ in the IR spectra of complexes 1-5, indicating the coordination through the carbonyl oxygen. The bands due to the C-O stretching vibrations at 1280 cm⁻¹ of free 3-Br-5-Cl-saloH are found in the IR spectra of complexes 1-5 at 1308-1324 cm⁻¹, because of the coordination of the phenolato oxygen of the ligand. Finally, the presence of the α-diimines was confirmed by the characteristic bands assigned to the corresponding out-of-plane $\rho(C-H)$ vibrations at 724-767 cm⁻¹.³⁸ The findings from the IR spectroscopy are in agreement with the determined X-ray crystal structures.

The UV-vis spectra of the complexes were recorded in the solid state as nujol mulls and in DMSO and buffer solutions (150 mM NaCl and 15 mM trisodium citrate at pH values 6–8, regulated by HCl solution). No significant changes (shift of the $\lambda_{\rm max}$ or new peaks) were observed in the spectra in the solid and liquid states, which is evidence that the complexes retain their structures in the pH range 6–8.

¹H NMR spectroscopy has also been used to confirm the binding of the 3-Br-5-Cl-salo ligand and α-diimines and the stability of the complexes in solution. The deprotonation of the phenol hydrogen is inferred by the absence of the –OH signal, which appears as a broad peak at δ = 12 ppm in the ¹H NMR spectrum of the free ligand. The ¹H NMR spectra of the complexes give signals attributable to the aldehyde proton at δ ~9.50 ppm. All sets of signals related to the presence of the ligands in the corresponding compounds are present; three for

Dalton Transactions Paper

the 3-Br-5-Cl-salo and four for the α -diimine ligands. All signals are slightly shifted downfield as expected upon binding to the zinc ion. Therefore, the ¹H NMR spectra are consistent with the obtained structures of 1-5.

The ¹H NMR spectra were also recorded for different time intervals (0, 24 and 72 h) and remained unchanged (representatively shown for complex 2 in Fig. S1†). The absence of an additional set of signals related to the dissociated ligands suggests that all complexes remain intact in solution. This fact in combination with the stability of UV-vis spectra in solution, the non-dissociation of the DMSO solutions and the formation of stable chelate rings upon coordination of the 3-Br-5-Cl-salo ligands and the α -diimine co-ligands with zinc(II) may reveal that the complexes remain intact in solution during the time necessary for the reported biological studies.

3.2 Structures of the complexes

3.2.1 Crystal structures of complexes 1 and 3. Single-crystals were obtained for complexes 1 and 3 and their structures were determined by X-ray crystallography. The molecular structures with the atom numbering schemes are presented in Fig. 2, while selected bond distances and angles are cited in Tables 1 and 2.

Table 1 Selected bond distances (Å) and bond angles (°) for complex 1

Bond	Distance (Å)	Bond	Distance (Å)
Zn1-O1	2.095(3)	Zn1-O4	2.042(3)
Zn1-O2	2.019(3)	Zn1-O5	2.106(3)
Zn1-O3	2.067(3)	Zn1-O6	2.099(3)
Bonds	Angle (°)	Bonds	Angle (°)
O1-Zn1-O2	87.14(13)	O2-Zn1-O3	175.46(13)
O1-Zn1-O3	88.81(13)	O2-Zn1-O4	96.23(13)
O1-Zn1-O4	175.69(12)	O2-Zn1-O5	94.99(13)
O1-Zn1-O5	85.75(13)	O2-Zn1-O6	93.77(14)
O1-Zn1-O6	87.20(13)	O4-Zn1-O5	91.26(13)
O3-Zn1-O4	87.92(13)	O4-Zn1-O6	95.24(13)
O3-Zn1-O5	86.75(13)	O5-Zn1-O6	168.47(13)
O3-Zn1-O6	83.98(13)		,

Complex 1 is a mononuclear zinc(II) complex (Fig. 2(A)), which consists of two deprotonated 3-Br-5-Cl-salo ligands lying at the equatorial sites and two aqua ligands occupying the apical sites, completing thus the distorted octahedron around the Zn(II) ion $(ZnO_6$ coordination sphere). The two 3-Br-5-Cl-salo ligands are coordinated to zinc(II) in a bidentate chelating mode through their carbonyl oxygen (O1, O3) and their phenolato (O2, O4) oxygen atoms with the Zn-Ocarbonvl

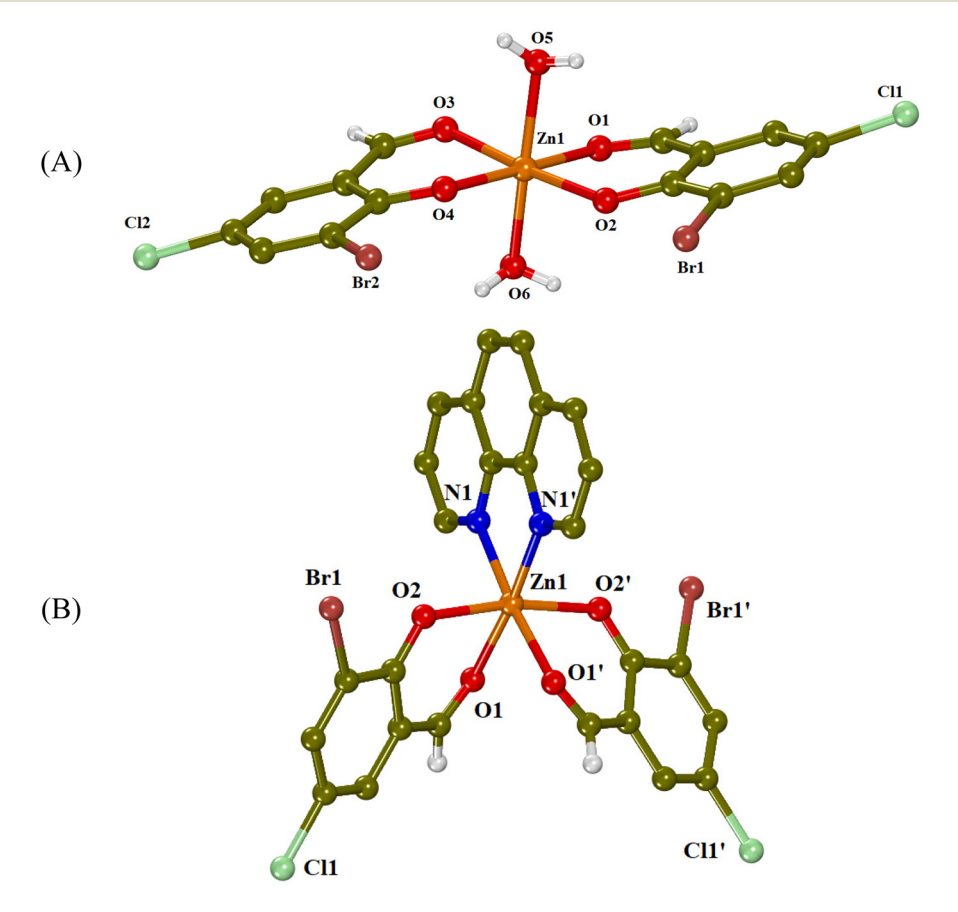


Fig. 2 Crystal structures of (A) complex 1 and (B) complex 3 (symmetry code: (') -x + 1, y, -z + 3/2). Aromatic hydrogen atoms are omitted for clarity.

·

Table 2 Selected bond distances (Å) and bond angles (°) for complex 3

Bond	Distance (Å)	Bond	Distance (Å)	
Zn1-O1 Zn1-O2	2.153(3) 2.036(3)	Zn1-N1	2.115(4)	
Bonds	Angle (°)	Bonds	Angle (°)	
O1-Zn1-O1 ⁱ 87.97(18) O1-Zn1-O2 84.47(12) O1-Zn1-O2 ⁱ 88.03(12) O1-Zn1-N1 96.39(13) O1-Zn1-N1 ⁱ 174.61(15)		O2-Zn1-O2 ⁱ O2-Zn1-N1 O2-Zn1-N1 ⁱ N1-Zn1-N1 ⁱ	169.58(15) 95.52(12) 92.50(12) 79.4(2)	

Symmetry code: (i) -x + 1, y, -z + 3/2.

Paper

distances being slightly longer than the Zn– $O_{phenolato}$ distances (Table 1) as expected and in accordance with the literature. ²⁵

The crystal structure of complex 1 is further stabilized by intermolecular hydrogen bonds between the aqua hydrogen atoms and phenolato oxygen atoms O2 and O4 of neighboring molecules (Table S2†).

In complex 3 (Fig. 2(B)), the Zn(II) ion has a ZnN₂O₄ coordination sphere, which consists of two deprotonated 3-Br-5-Cl-salo⁻ ligands, coordinated in a bidentate chelating mode through their carbonyl (O1) and phenolato (O2) oxygen atoms, and a chelating phen ligand bound through its nitrogen atoms. The phenolato oxygen atoms are in *trans* positions to each other, with an O2ⁱ–Zn1–O2 angle of 169.58(15)° and the carbonyl oxygens are at *cis* positions, with an O1ⁱ–Zn1–O1 angle of 87.97(18)° (Table 2). This kind of arrangement is often found in [M(X–salo)₂(α -diimine)] complexes.²⁴

3.2.2 Proposed structures for complexes 2, 4 and 5. Based on the findings of IR, 1H NMR and UV-vis spectroscopy, elemental analysis and molar conductivity measurements, and from the comparison of the crystal structure of complex 3 with those of other similar mixed-ligand zinc(II) complexes found in the literature, 25 we may suggest that complexes 2, 4 and 5 are neutral, mononuclear, with coordination number six and present octahedral geometry; the two deprotonated 3-Br-5-Cl-salo ligands are bidentately bound to Zn(II) through the carbonyl and phenolato oxygen atoms, and the corresponding α -diimine is coordinated to zinc(II) through its nitrogen atoms.

3.3 Study of the biological profile of the complexes

A number of different studies have been performed in order to screen the biological profile of 3-Br-5-Cl-saloH and its complexes 1–5. These studies may give insight into how the complexes interact with DNA and serum albumins and help investigate their antioxidant and antimicrobial properties.

The study of the interaction of coordination complexes with DNA is important, since DNA is often a key target for the development of anticancer drugs and antibacterial agents, which owe their properties to the interaction with DNA and/or the induction of DNA cleavage.³⁹ When a compound can interact with DNA, it should also be able to get transported to reach its potential target. Serum albumins usually play the role of trans-

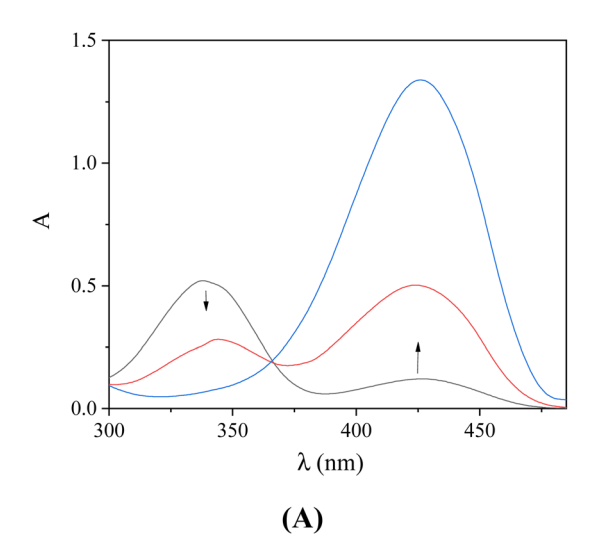
porting drugs and/or bioactive compounds towards the environment of the biological targets; therefore, it is of vital importance to study the interactions of bioactive compounds with such proteins. The investigation of the binding strength and the mechanism of interaction of small molecules with serum albumins is important for the clarification of the pharmacodynamics and pharmacokinetics, as they play an important role in drug absorption, distribution, metabolism and excretion. BSA is usually selected as a relevant model, because of its structural similarity to human serum albumin (76%), its low cost and easy availability. However, the report on plasma protein binding is now an FDA requirement in screening potential therapeutic agents, so the study of the interaction with HSA is also important.

Coordination compounds may also serve as an alternative to traditional synthetic antioxidants, because of their variety in coordination number, different geometries and oxidation states, which facilitates and favors the redox processes associated with their antioxidant action. But this variety also makes coordination compounds very useful in accessing another highly underexplored chemical space for drug development, the design of new antimicrobial agents. Metal complexes have exhibited noteworthy antimicrobial activity as a result of synergism with antimicrobial ligands. Metal complexes could lead to exchange or release of ligands, redox activation, catalytic generation of reactive oxygen species (ROS) and depletion of essential substrates making them able to stop enzymatic activities, inhibit membrane function or induce DNA damage in microbes.

3.3.1 Interaction with calf-thymus DNA. Metal complexes may interact with DNA by various modes. In covalent interaction, at least one labile ligand of the complex is replaced by the nitrogen of a DNA-base pair. Non-covalent interactions involve: (i) intercalation as a result of π - π stacking interactions between the complexes and DNA-base pairs, (ii) electrostatic interaction outside the helix attributed to Coulomb forces and (iii) groove-binding due to the development of van der Waals forces, hydrogen bonding, and hydrophobic interactions with the major or minor DNA-groove. ^{43,44} Cleavage of DNA may also appear when the compounds act as nucleases. The interaction of the compounds (3-Br-5-Cl-saloH and complexes 1–5) with CT DNA was investigated by UV-vis spectroscopy, DNA viscosity measurements and *via* competitive studies with EB monitored by fluorescence emission spectroscopy.

UV-vis spectroscopy is used initially to study the interaction between a compound and CT DNA and to estimate its binding strength, since any interaction between DNA and the compound may perturb the band(s) observed in the spectra. ⁴⁵ For this reason, the UV-vis spectra of the compounds (10^{-4} M) were recorded in the presence of increasing amounts of CT DNA (Fig. 3 and S2†) and the changes of the $\lambda_{\rm max}$ were recorded. In the UV-vis spectra of the compounds, two bands are observed: band I located at around 309–340 nm and band II at 413–427 nm. Upon addition of CT DNA, medium-to-intense hypochromism is observed for band I accompanied by a red-shift, while band II exhibits only hyperchromism

Dalton Transactions Paper



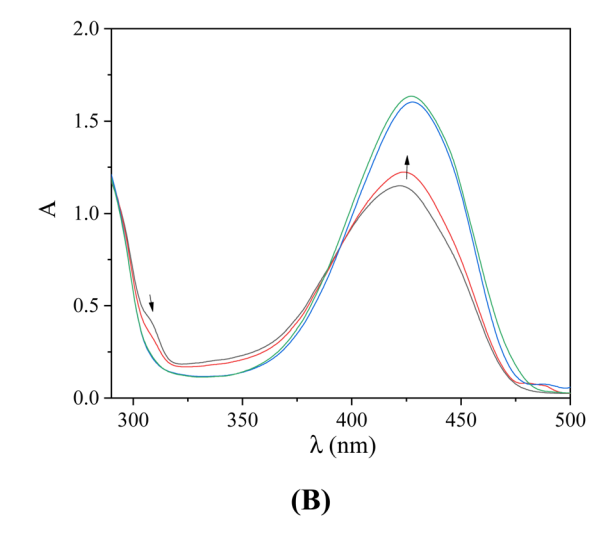


Fig. 3 UV-vis spectra of DMSO solution (10⁻⁴ M) of (A) 3-Br-5-Cl-saloH and (B) complex 2, in the presence of increasing incremental amounts of CT DNA (10⁻⁴ M). The arrows show the changes upon increasing amounts of CT DNA.

Table 3 Spectral features of the UV-vis spectra of the compounds upon addition of CT DNA. UV-vis band (λ_{max} in nm) (percentage of hyper-/hypo-chromism ($\Delta A/A_0$, %), blue-/red-shift of the $\lambda_{max}(\Delta \lambda$, in nm) and the corresponding DNA-binding constants (K_b , M^{-1})

Compound	Band $(\Delta A/A_0 (\%)^a, \Delta \lambda (nm)^b)$	$K_{\rm b} \left(\mathbf{M}^{-1} \right)$
3-Br-5-Cl-saloH Complex 1 Complex 2 Complex 3 Complex 4 Complex 5	338(<-50, elim'); 427(>+50, 0) 338(-27, elim); 413(>+50, +10) 309(<-50, elim); 422(+39, +5) 325(<-50, elim); 422(+45, +5) 329(<-20, 0); 418(+47, +10) 337(-48, +13); 425(>+50, 0)	$\begin{aligned} &1.13(\pm0.08)\times10^4\\ &1.10(\pm0.21)\times10^6\\ &6.74(\pm0.08)\times10^5\\ &7.16(\pm0.08)\times10^5\\ &1.18(\pm0.08)\times10^6\\ &4.31(\pm0.08)\times10^6\end{aligned}$

a "+" denotes hyperchromism and "-" denotes hypochromism. b "+" denotes red-shift and "-" denotes blue-shift. "elim" denotes elimination of the band.

(Table 3). These changes may suggest the binding of the complexes to CT DNA, 46 although sufficient evidence of the interaction mode with DNA cannot be obtained. For this purpose, DNA viscosity measurements and EB-competitive studies were conducted.

In order to estimate the binding strength of the compounds to CT-DNA, the DNA-binding constants (K_b) of the compounds were calculated with the Wolfe-Shimer equation (eqn (S1)†)⁴⁷ and the plots [DNA]/ $(\varepsilon_A - \varepsilon_f)$ versus [DNA] (Fig. S3†). All complexes 1-5 are tighter DNA-binders than free 3-Br-5-Cl-saloH with complex 5 presenting the highest K_b constant (Table 3). The K_b constants of complexes 1–5 (Table 3) are relatively high (of the order $10^5 – 10^6 \,\mathrm{M}^{-1}$) and higher than that of the classical intercalator EB (= $1.23(\pm 0.07) \times 10^5 \text{ M}^{-1}$). The K_b constants are similar to other zinc(II)-salicylaldehyde complexes found in the literature. 11,24,25

In order to further investigate the interaction of the compounds with CT DNA, the changes of the viscosity of a DNA solution in the presence of the compounds were monitored, since the viscosity of DNA is usually related to its length

changes, induced by the interaction with a compound. An increase in DNA-viscosity may be interpreted as intercalation, since the distance between the DNA-base pairs gets longer, which leads to an increase in the relative DNA-length. In the case of interaction on the DNA surface (i.e., non-classical intercalation), the relative DNA-length does not change significantly and a negligible decrease in the DNA-viscosity may be observed.49

The DNA-viscosity measurements were carried out on CT DNA solutions (0.1 mM) by adding increasing amounts of the compounds (up to the value of r = 0.36) at room temperature. The relative viscosity of DNA exhibited an increase upon addition of the compounds (Fig. 4). In particular, all complexes exhibited a higher initial increase in their relative DNAviscosity than the free 3-Br-5-Cl-saloH. The observed behavior

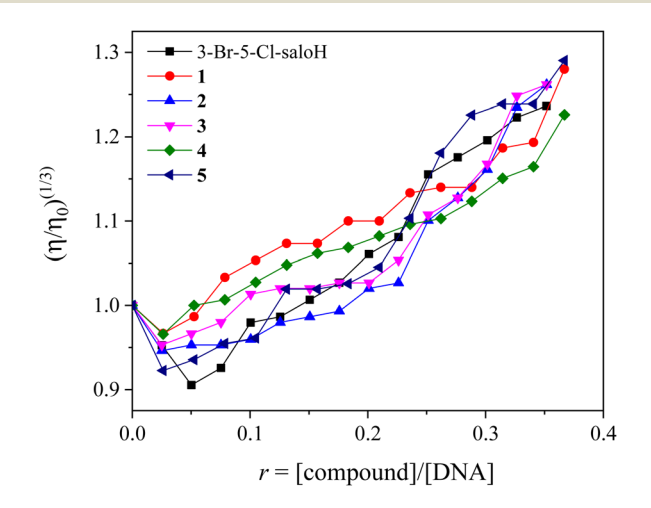


Fig. 4 Relative viscosity $(\eta/\eta_0)^{1/3}$ of CT DNA (0.1 mM) in buffer solution (150 mM NaCl and 15 mM trisodium citrate at pH 7.0) in the presence of increasing incremental amounts of the compounds (r = 0-0.36).

This article is licensed under a Creative Commons Attribution 3.0 Unported Licence.

Open Access Article. Published on 07 November 2022. Downloaded on 12/14/2025 4:07:13 PM.

Paper

of the DNA-viscosity may be considered evidence of the existence of an intercalative interaction mode with DNA clarifying thus the UV-vis spectroscopic features.

In order to further investigate the interaction of the compounds with CT DNA, competitive studies with the typical intercalator EB were carried out. A solution containing the EB-DNA conjugate shows an intense fluorescence emission band at 592 nm (with $\lambda_{\text{excitation}} = 540 \text{ nm}$) as a result of the intercalation of the planar EB-phenanthridine ring in-between adjacent DNA-base pairs. For this reason, EB is considered a typical indicator of DNA-intercalation.⁵⁰ If a compound that intercalates to DNA equally or stronger than EB is added into this solution, significant quenching of the EB-DNA fluorescence emission may be observed. The compounds do not show any fluorescence emission bands at room temperature in solution or in the presence of CT DNA or EB under the same experimental conditions ($\lambda_{ex} = 540 \text{ nm}$).

The fluorescence emission spectra of a pre-treated solution containing the EB-DNA adduct ([EB] = $20 \mu M$, [DNA] = $26 \mu M$) were recorded in the presence of increasing amounts of each compound up to the value of r = 0.45 (representatively shown for complex 3 in Fig. 5(A)). The addition of the compounds resulted in a notable quenching of the fluorescence emission band at 592 nm (which was up to 53.4% for complex 2 of the initial EB-DNA fluorescence, Fig. 5(B) and Table 4). Therefore, the induced quenching may indicate the ability of the compounds to displace EB from the EB-DNA adduct, revealing indirectly the interaction with CT DNA by the intercalative mode. 50,51

The K_{SV} constants (Table 4) of the compounds were calculated with the Stern-Volmer equation (eqn (S2)†)⁵⁰ and the Stern-Volmer plots (Fig. S4 \dagger). The values of K_{SV} were found relatively high, which is an indication of a tight binding of the

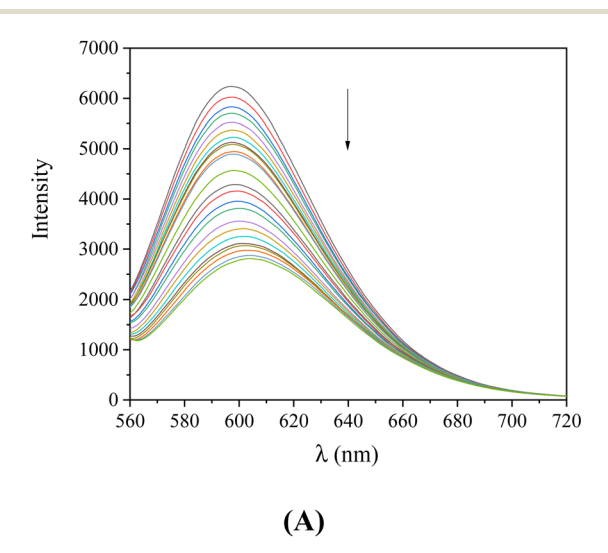
Table 4 Percentage of EB-DNA fluorescence quenching $(\Delta I/I_0, \%)$ and the Stern-Volmer (K_{SV} in M^{-1}) and EB-DNA quenching constants (k_{q_1} M^{-1} s⁻¹) for the compounds

Compound	$\Delta I/I_0\left(\%\right)$	$K_{\mathrm{SV}}\left(\mathbf{M}^{-1}\right)$	$k_{\rm q} \left({ m M}^1 \ { m s}^{-1} ight)$
3-Br-5-Cl-saloH Complex 1 Complex 2 Complex 3 Complex 4 Complex 5	45.1 44.6 53.4 49.2 52.4 48.4	$\begin{array}{c} 2.86(\pm 0.07) \times 10^4 \\ 3.40(\pm 0.10) \times 10^4 \\ 4.16(\pm 0.06) \times 10^4 \\ 3.40(\pm 0.06) \times 10^4 \\ 5.36(\pm 0.18) \times 10^4 \\ 3.33(\pm 0.08) \times 10^4 \end{array}$	$\begin{array}{c} 1.24(\pm0.03)\times10^{13}\\ 1.48(\pm0.04)\times10^{12}\\ 1.81(\pm0.02)\times10^{12}\\ 1.43(\pm0.03)\times10^{12}\\ 2.33(\pm0.08)\times10^{12}\\ 1.45(\pm0.04)\times10^{12}\\ \end{array}$

complexes to DNA. Complex 4 exhibits the highest K_{SV} constant among the complexes. The reported constants are of the same magnitude as those found for zinc complexes of salicylaldehydes. 11,24,25 The EB-DNA quenching constants of the compounds (k_q) were calculated with eqn (S3)† (considering τ_0 = 23 ns as the fluorescence lifetime of the EB-DNA system).52 A piece of evidence that the quenching of the EB-DNA fluorescence takes place via a static mechanism can be deduced from the fact that the values of the k_{q} constant of the compounds (Table 4) were found higher than 10¹⁰ M⁻¹ s⁻¹.⁵¹

From all the above experiments (UV-Vis titration studies, viscosity measurements and competitive studies with EB), it can be concluded that 3-Br-5-Cl-saloH and its complexes 1-5 interact with CT DNA via an intercalative mode and present relatively strong binding ability.

3.3.2 Interaction with pBR322 plasmid DNA. In order to investigate the potential nuclease-like ability of the compounds, the cleavage of pBR322 plasmid DNA (pDNA) by the compounds was examined by the agarose gel electrophoresis technique. The supercoiled pDNA in an agarose gel during electrophoresis is shown as form I (Fig. 6, lane 1). The com-



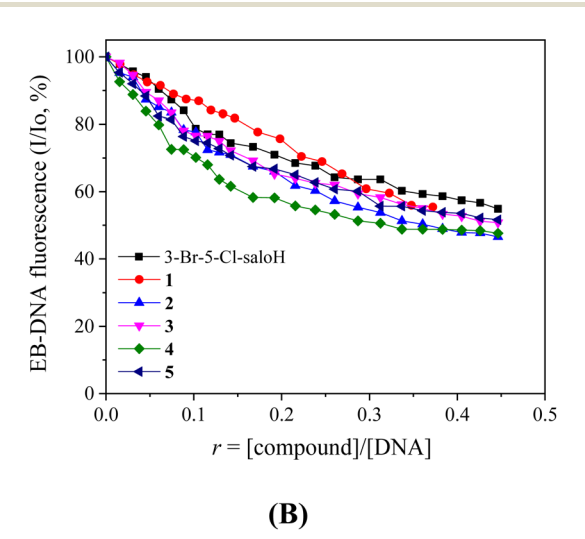


Fig. 5 (A) Fluorescence emission spectra ($\lambda_{\rm exc}$ = 540 nm) for the EB-DNA conjugate ([EB] = 20 μ M, [DNA] = 26 μ M) in buffer solution (150 mM NaCl and 15 mM trisodium citrate at pH = 7.0) in the absence and in the presence of increasing incremental amounts of complex 3 (up to r = 0.45). The arrow shows the changes of intensity upon increasing amounts of complex 3. (B) Plot of the EB-DNA relative fluorescence emission intensity at $\lambda_{\text{emission}} = 592 \text{ nm}$ (%) versus r (r = [compound]/[DNA]) in the presence of the compounds (up to 54.9% of the initial EB-DNA fluorescence emission intensity for 3-Br-5-Cl-saloH, 55.4% for complex 1, 46.6% for complex 2, 50.8% for complex 3, 47.6% for complex 4 and 51.6% for complex 5).

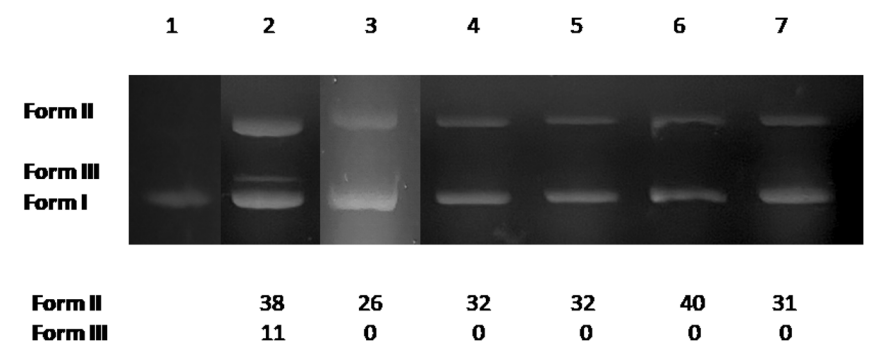


Fig. 6 Agarose gel electrophoretic pattern of EB-stained plasmid DNA (pBR322 plasmid DNA, 50 μM/base pair) with 3-Br-5-Cl-saloH and its complexes 1–5 (at 500 μM). Top: gel electrophoresis pictures: lane 1: DNA; lane 2: DNA + 3-Br-5-Cl-saloH; lane 3: DNA + complex 1; lane 4: DNA + complex 2; lane 5: DNA + complex 3; lane 6: DNA + complex 4; lane 7: DNA + complex 5. Bottom: calculation of the % conversion to ss and ds damage. DNA forms: form I = supercoiled, form II = relaxed, and form III = linear plasmid DNA. Power supply: 65 V for 1 h.

pounds (final concentration of 500 μ M in DMSO solution) were mixed with pDNA (Tris buffer solution, 25 μ M, pH = 6.8). The amount of DMSO within the final mixture did not exceed 10% v/v. After incubation of the components for 30 min at 37 °C, pDNA was analyzed by gel electrophoresis on 1% agarose stained with EB.

The potential DNA-cleaving activity by complexes 1–5 (Fig. 6, lanes 3–7) was revealed as single-stranded (ss) nicks in the supercoiled DNA forming relaxed circular DNA (form II), while an additional double-stranded (ds) nick was revealed for 3-Br-5-Cl-saloH (Fig. 6, lane 2) leading to the formation of linear DNA (form III). The percentages of ss and ds shown in Fig. 6 were calculated with eqn (S4) and (S5).† At a high concentration of 500 μ M, the compounds present moderate DNA-cleaving activity up to 40% (Fig. 6, lane 6, for complex 4) which is slightly higher than their Zn(II) analogues with 3,5-dibromosalicylaldehyde and 3,5-dichloro-salicylaldehyde. 11,24

3.3.3 Interaction with serum albumins. Serum albumins are important proteins of the circulatory system and are the carriers of drugs and other bioactive small molecules through the bloodstream. BSA is the most widely studied albumin and is structurally homologous to HSA, possessing two and one tryptophan residues, respectively. When their solutions are excited at 295 nm, intense fluorescence emission bands with $\lambda_{\rm em,max}=342$ nm for BSA and 350 nm for HSA are observed, respectively, because of the tryptophan residues. The solutions of complexes 1–5 exhibited the maximum emission in the region 395–415 nm under the same experimental conditions and in such cases the SA-fluorescence emission spectra were corrected before the calculation process. The inner-filter effect was found rather low, minimally affecting the measurements and was calculated with eqn (S6). † 55

When the compounds (10^{-4} M) were added incrementally into a SA solution $(3 \mu\text{M})$, a significant quenching of the fluorescence emission bands of the albumins at $\lambda_{em} = 340-345$ nm was observed and the quenching induced by the compounds was less pronounced in the case of HSA (Fig. 7). The observed quenching can be attributed to the changes in the tryptophan environment of the albumins, due to the possible denatura-

tion of their secondary structure, resulting from the binding of the compounds to SA. 56

The SA-quenching constants $(k_{\rm q})$ of the compounds (Table 5) (calculated from the corresponding Stern–Volmer plots (Fig. S5 and S6†) and the Stern–Volmer quenching equations (eqn (S2) and (S3)†)) are much higher than $10^{10}~{\rm M}^{-1}~{\rm s}^{-1}$, which is an indication of a static quenching mechanism³⁹ and verifies the interaction of the compounds with the albumins, with complexes 3 and 1 presenting the highest $k_{\rm q}$ constants for BSA and HSA, respectively. The $k_{\rm q}$ constants of complexes 1–5 are similar to those reported for similar Zn(II) with substituted salicylaldehydes as ligands. 11,24,25

The SA-binding constants (K) of the compounds (calculated from the corresponding Scatchard plots (Fig. S7 and S8†) and the Scatchard equation (eqn (S7)†)) (Table 5) are relatively high. This implies a tight interaction of the compounds with the albumins, which allows them to get transported towards the environment of their potential biological targets. The K values were found significantly lower than the constant of avidin (which is of the order $10^{15}~{\rm M}^{-1}$ and is regarded as the limit between the reversible and irreversible interactions), so a reversible interaction of the complexes with serum albumins may be assumed, and the complexes may get released when they approach close to the environment of their targets. Tomplex 1 exhibited the highest K constants for both albumins among the complexes.

3.3.4 Antioxidant activity of the compounds. Free radicals can cause inflammations.⁵⁸ Antioxidants are compounds that can neutralize free radicals and are usually organic compounds such as phenolic and cinnamic acids, flavones, flavonoids, *etc*. The carboxylic group in these acids or a near hydroxyl group and an oxo group enables them to coordinate to metal ions through their oxygen atoms, and form stable complexes. An interesting method to develop antioxidant compounds is to combine the redox properties of metal ions with various ligands.⁴²

The DPPH-radical assay was developed in the 1950s and has often been used to assess the antioxidant capacity of several metal complexes. 42 It correlates to ageing prevention

Paper

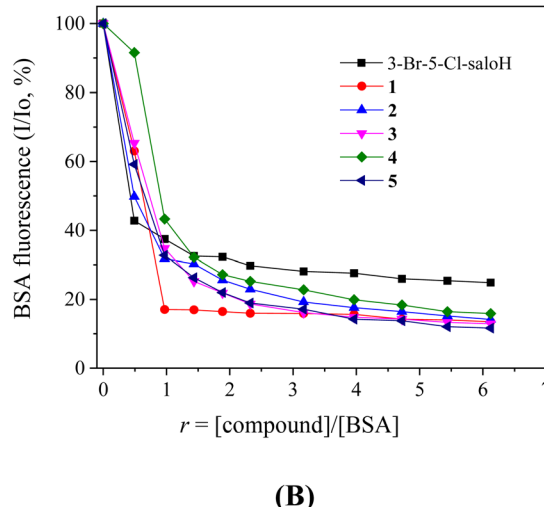


Fig. 7 (A) Plot of % relative HSA-fluorescence emission intensity at $\lambda_{em} = 340$ nm (%) vs. r (r = [complex]/[HSA]) for the compounds (up to 42.7% of the initial HSA fluorescence for 3-Br-5-Cl-saloH, 13.5% for complex 1, 39.6% for complex 2, 25.3% for complex 3, 29.0% for complex 4, and 23.0% for complex 5 in buffer solution (150 mM NaCl and 15 mM trisodium citrate at pH 7.0). (B) Plot of % relative BSA-fluorescence emission intensity at $\lambda_{em} = 345$ nm (%) vs. r (r = [complex]/[BSA]) for the compounds (up to 24.9% for 3-Br-5-Cl-saloH, 13.5% for 1, 14.1% for 2, 12.9% for 3, 15.8% for 4 and 11.6% for 5) in buffer solution (150 mM NaCl and 15 mM trisodium citrate at pH 7.0).

Table 5 The BSA- and HSA-quenching (k_q) and binding constants (K) for the compounds

(A)

Compound	$k_{ m q(BSA)} ({ m M}^{-1} { m s}^{-1})$	$K_{(\mathrm{BSA})}\left(\mathbf{M}^{-1}\right)$	$k_{\rm q(HSA)} ({ m M}^{-1} { m s}^{-1})$	$K_{(\mathrm{HSA})}\left(\mathbf{M}^{-1}\right)$
3-Br-5-Cl-saloH Complex 1 Complex 2 Complex 3 Complex 4 Complex 5	$1.36(\pm 0.10) \times 10^{13}$ $3.97(\pm 0.12) \times 10^{13}$ $2.58(\pm 0.11) \times 10^{13}$ $5.85(\pm 0.34) \times 10^{13}$ $2.24(\pm 0.08) \times 10^{13}$ $3.54(\pm 0.15) \times 10^{13}$	$\begin{array}{c} 1.44(\pm 0.07) \times 10^6 \\ 3.49(\pm 0.25) \times 10^6 \\ 8.21(\pm 0.18) \times 10^5 \\ 1.02(\pm 0.04) \times 10^6 \\ 6.89(\pm 0.20) \times 10^5 \\ 8.64(\pm 0.22) \times 10^5 \end{array}$	$egin{array}{l} 1.83(\pm 0.11) imes 10^{13} \\ 4.38(\pm 0.15) imes 10^{13} \\ 6.55(\pm 0.28) imes 10^{12} \\ 1.80(\pm 0.10) imes 10^{13} \\ 1.21(\pm 0.06) imes 10^{13} \\ 1.83(\pm 0.09) imes 10^{13} \end{array}$	$\begin{array}{c} 1.26(\pm0.04)\times10^6\\ 3.45(\pm0.17)\times10^6\\ 4.62(\pm0.17)\times10^5\\ 5.55(\pm0.13)\times10^5\\ 2.87(\pm0.05)\times10^5\\ 3.23(\pm0.13)\times10^5\\ \end{array}$

and anti-cancer and anti-inflammation activities.⁵⁹ The ability to scavenge the cationic ABTS radicals (ABTS^{*†}) has often been used as a tool to measure the total antioxidant activity of a complex.⁴⁸ Finally, H₂O₂, which is generated *in vivo* by several oxidase enzymes and activated by phagocytes, helps in killing several bacterial and fungal strains and may serve as a messenger molecule in the synthesis and activation of several inflammatory mediators. When a scavenger is incubated with H₂O₂, using a peroxidase assay system, the loss of H₂O₂ can be measured.⁶⁰ For the above reasons, compounds able to sca-

venge free radicals or to inhibit their formation, may be found helpful in the treatment of inflammations.

Within this context, the antioxidant activity of the compounds was examined regarding the scavenging of DPPH and ABTS radicals and reduction of $\rm H_2O_2$ and was compared with that of the well-known antioxidant agents NDGA, BHT, Trolox and L-ascorbic acid, which are used as reference antioxidant agents. 61,62 The results are summarized in Table 6.

The DPPH-scavenging ability of the compounds was rather high and rather time-independent. The reported $zinc(\pi)$ com-

 $\textbf{Table 6} \quad \text{DPPH-scavenging ability (DPPH\%), ABTS-radical scavenging activity (ABTS\%), and H_2O_2 reducing activity ($H_2O_2\%)$ for the compounds $H_2O_2\%$ reducing $H_$

Compound	DPPH%, 30 min	DPPH%, 60 min	ABTS%	$\mathrm{H_2O_2}\%$
3-Br-5-Cl-saloH	52.79 ± 1.13	53.64 ± 0.83	14.52 ± 0.46	80.86 ± 0.77
Complex 1	55.25 ± 1.14	56.68 ± 1.77	27.50 ± 1.05	99.52 ± 0.43
Complex 2	59.98 ± 0.16	61.76 ± 0.13	46.20 ± 0.12	85.06 ± 1.49
Complex 3	53.83 ± 0.98	55.15 ± 1.34	72.58 ± 0.23	99.63 ± 0.10
Complex 4	52.38 ± 0.65	52.77 ± 1.06	52.19 ± 1.04	95.09 ± 0.64
Complex 5	54.99 ± 1.10	56.13 ± 1.30	59.06 ± 1.33	98.02 ± 0.25
NDGA	87.08 ± 0.12	87.47 ± 0.12	Not tested	Not tested
ВНТ	61.30 ± 1.16	79.78 ± 1.12	Not tested	Not tested
Trolox	Not tested	Not tested	98.10 ± 0.48	Not tested
L-Ascorbic acid	Not tested	Not tested	Not tested	60.80 ± 0.20

Dalton Transactions Paper

plexes were in most cases more active than 3-Br-5-Cl-saloH with complex 2 presenting the highest DPPH-scavenging activity, although lower than that of the reference compounds BHT and NDGA. All complexes were found to be more active ABTS-scavengers than free 3-Br-5-Cl-saloH, with complex 3 being the best ABTS-scavenger among the compounds. Concerning the reduction of H2O2, the complexes are more efficient than the free ligand and more than the reference compound L-ascorbic acid. Complexes 1 and 3 presented the highest reducing ability of H₂O₂.

In general, complexes 1-5 presented better antioxidant activity than free 3-Br-5-Cl-saloH, indicating that the coordination to zinc(II) ion improved the antioxidant ability of the free ligand. Compared with the analogous zinc(II) complexes of 3,5-diCl-saloH and 3,5-diBr-saloH, complexes 1-5 exhibited higher ability to scavenge DPPH and ABTS radicals and were found more active in reducing H₂O₂. 11,24,25

3.3.5 Antimicrobial activity of the compounds. Previous studies have shown that substituted salicylaldehydes may present significant antimicrobial properties, possibly because of the formation of Schiff bases with the amino groups of microbial cells. Substitution on the benzene ring seems to play an important role, since benzaldehyde and salicylaldehyde have been found to present low activity. However, the presence of halogens, the hydroxy group or the nitro group could result in compounds with higher activity. Unfortunately, this activity cannot be predicted and could be different for each microbe. 7,8 Previous studies regarding the zinc(II) complexes of (bis)halogenated-substituted salicylaldehydes (3,5-dibromo-salicylaldehyde and 3,5-dichloro-salicylaldehyde) showed that the complexes presented interesting antimicrobial properties. 11,24

In an effort to further clarify the nature of halogen-substitution on the benzene ring, the in vitro antimicrobial activity of the compounds was examined against two Gram-positive microorganisms (S. aureus and B. subtilis) and two Gram-negative microorganisms (E. coli and X. campestris), and the corresponding MIC values were determined. The results are found in Table 7.

3-Br-5-Cl-saloH presented equal antimicrobial activity against all tested microorganisms (MIC = 100 µg mL⁻¹) but lower than 3,5-dibromo-salicylaldehyde (MIC = $25-50 \mu \text{g mL}^{-1}$) and 3,5-dichloro-salicylaldehyde (MIC = 50 μ g mL⁻¹)^{11,24} against the same microorganisms suggesting that the combination of two different halogens leads to lower activity.

Complexes 1-5 presented better results against Gram(+) microorganisms and complexes 4 and 5 presented the best

Table 7 Antimicrobial activity of the compounds expressed in MIC (in $\mu g m L^{-1}$ or μM (the values in parentheses))

-				
Compound	X. campestris	E. coli	B. subtilis	S. aureus
3-Br-5-Cl-saloH	100 (425)	100 (425)	100 (425)	100 (425)
Complex 1	200 (351)	>200 (>351)	50 (88)	100 (175)
Complex 2	200 (290)	>200 (>290)	50 (72)	100 (144)
Complex 3	100 (140)	50 (70)	50 (70)	50 (70)
Complex 4	200 (269)	50 (67)	25 (34)	50 (67)
Complex 5	200 (284)	100 (142)	25 (35)	50 (71)

activity with regard to B. subtilis (MIC = 25 $\mu g \text{ mL}^{-1}$). Compared with their analogous zinc(II) complexes with 3,5-diCl-saloH or 3,5-diBr-saloH, complexes 1-5 presented lower antimicrobial activity in accordance with the corresponding saloH ligands, 11,24 so as a premature conclusion, we could say that the use of two different halogens in the benzene ring did not seem to improve the antimicrobial properties of the complexes, but further studies need to be performed.

Conclusions

Five zinc(II) complexes of 3-Br-5-Cl-salicylaldehyde were prepared and characterized by various techniques. The crystal structures of complexes 1 and 3 were determined by singlecrystal X-ray crystallography, revealing the bidentate coordination of the ligand to the metal ion. The complexes may interact with CT DNA via intercalation and the highest DNAbinding constant was found for complex 5 [Zn(3-Br-5-Cl-salo)₂ (bipyam)] $(K_b = 4.31(\pm 0.08) \times 10^6 \text{ M}^{-1})$. The complexes can moderately cleave pBR322 plasmid DNA to relaxed circular DNA (up to 40%) at a concentration of 500 μM. The complexes may bind tightly and reversibly to bovine and human serum albumin. Concerning the antioxidant activity of the compounds, all complexes 1-5 exhibited noteworthy scavenging ability of DPPH radicals (DPPH% = 52.38-61.76%), and significant ABTS-scavenging activity up to 72.58%. Almost all complexes 1-5 exhibited very high ability to reduce H₂O₂ (up to 99.63%), which constitutes a promising conclusion regarding their potential applications in the future. The antimicrobial activity of complexes 1-5 against two Gram-negative (X. campestris and E. coli) and two Gram-positive (B. subtilis and S. aureus) bacterial strains was tested. The activity of the complexes against the Gram(-) bacteria tested was low and the complexes were found to be more active against Gram(+) microorganisms; in particular, the best MIC values were determined for complexes 4 and 5 against B. subtilis.

A plethora of different studies were employed to investigate the biological profile of 3-Br-5-Cl-saloH and its complexes 1-5. The tight intercalative binding of the complexes with CT DNA and the potential cleavage of plasmid DNA induced by the complexes in combination with the noteworthy antioxidant potency (scavenging of free radicals and reduction of hydrogen peroxide) may serve as the first indicative step towards anticancer activity. The reported antimicrobial activity may also be interconnected with DNA-binding and the DNA-cleavage properties of the complexes, as there are numerous commonly used antibacterial drugs (e.g. quinolones) that target bacterial DNA and/or the inhibition of enzymes related to the replication of DNA (e.g. topoisomerases and DNA-gyrases). In all cases, the role of serum albumins should also be taken into consideration for biological studies mainly due to their role as carriers of drugs and/or bioactive compounds towards the environment of their biological targets, although in some cases it is difficult for the albumins to approach too close to such targets (e.g. in the case of nuclear DNA).

Paper **Dalton Transactions**

The combination of different techniques may provide not only preliminary information of the biological potency of the compounds but also important evidence of how the complexes interact with DNA and serum albumins and of their antioxidant and antimicrobial properties, increasing future prospects for further studies of their biological properties with the employment of more elaborate experiments regarding their potential use as pharmaceutical agents.

Abbreviations

3-Br-5-Cl-3-bromo-5-chloro-salicylaldehyde

saloH

ABTS 2,2'-Azinobis(3-ethylbenzothiazoline-6-sulfonic

acid

B. subtilis Bacillus subtilis ATCC 6633

bipy 2,2'-Bipyridine bipyam 2,2'-Bipyridylamine **BSA** Bovine serum albumin

CTCalf-thymus

DPPH 1,1-Diphenyl-picrylhydrazyl

ds Double-stranded

E. coli Escherichia coli NCTC 29212

EBEthidium bromide, 3,8-diamino-5-ethyl-6-

phenyl-phenanthridinium bromide

HSA Human serum albumin K SA-binding constant $K_{\rm b}$ **DNA-binding** constant Quenching constant $k_{\rm q}$ Stern-Volmer constant K_{SV}

MIC Minimum inhibitory concentration

NDGA Nordihydroguaiaretic acid

Neoc 2,9-Dimethyl-1,10-phenanthroline, neocuproine

pDNA Supercoiled circular pBR322 plasmid DNA

1,10-Phenanthroline phen

[Compound]/[DNA] ratio [compound]/

[albumin] ratio

Staphylococcus aureus ATCC 6538 S. aureus

Serum albumin SA SS Single-stranded

Trolox 6-Hydroxy-2,5,7,8-tetramethylchromane-2-car-

boxylic acid

Xanthomonas campestris ATCC 1395 Χ.

campestris

Conflicts of interest

There are no conflicts to declare.

Acknowledgements

AZ has received a postdoctoral scholarship for this research which is co-financed by Greece and the European Union

(European Social Fund - ESF) through the Operational Programme "Human Resources Development, Education and Lifelong Learning" in the context of the project "Reinforcement of Postdoctoral Researchers - 2nd Cycle" (MIS-5033021), implemented by the State Scholarships Foundation

References

- 1 A. Jayamani, R. Bellam, G. Gopu, S. O. Ojwach and N. Sengottuvelan, Polyhedron, 2018, 156, 138-149.
- 2 J. A. Lee, M. T. Uhlik, C. M. Moxham, D. Tomandl and D. J. Sall, J. Med. Chem., 2012, 55, 4527-4538.
- 3 C. H. Ng, K. C. Kong, S. T. Von, P. Balraj, P. Jensen, E. Thirthagiri, H. Hamada and M. Chikira, Dalton Trans., 2008, 4, 447-454.
- 4 A. I. Matesanz, C. Hernandez, A. Rodriguez and P. Souza, Dalton Trans., 2011, 40, 5738-5745.
- 5 M. Claudel, J. V. Schwarte and K. M. Fromm, Chemistry, 2020, 2, 849-899.
- 6 G. Pauls, T. Becker, P. Rahfeld, R. R. Gretscher, C. Paetz, J. Pasteels, S. H. von Reuss, A. Burse and W. Boland, J. Chem. Ecol., 2016, 42, 240-248.
- 7 E. Pelttari, E. Karhumaki, J. Langshaw, H. Perakyla and H. Elo, Z. Naturforsch., C: J. Biosci., 2007, 62, 487-497.
- 8 E. Pelttari, M. Lehtinen and H. Elo, Z. Naturforsch., C: J. Biosci., 2011, 66, 571-580.
- 9 H. Elo, M. Kuure and E. Pelttari, Eur. J. Med. Chem., 2015, 92, 750-753.
- 10 S. Ntanatsidis, S. Perontsis, S. Konstantopoulou, S. Kalogiannis, A. G. Hatzidimitriou, A. N. Papadopoulos and G. Psomas, J. Inorg. Biochem., 2022, 227, 111693.
- E. Geromichalou, G. Geromichalos, Zianna, A.-M. Fiotaki, A. G. Hatzidimitriou, S. Kalogiannis and G. Psomas, J. Inorg. Biochem., 2022, 226, 111659.
- 12 A. Zianna, G. Geromichalos, A.-M. Fiotaki, A. G. Hatzidimitriou, S. Kalogiannis and G. Psomas, Pharmaceuticals, 2022, 15, 886.
- 13 S. Parveen, K. Fatima, S. Zehra and F. Arjmand, J. Biomol. Struct. Dyn., 2021, 39, 6070-6083.
- 14 N. Kordestani, H. A. Rudbari, A. R. Fernandes, L. R. Raposo, P. V. Baptista, D. Ferreira, G. Bruno, G. Bella, R. Scopelliti, J. D. Braun, D. E. Herbert and O. Blacque, ACS Comb. Sci., 2020, 22, 89-99.
- 15 M. Jarosz, M. Olbert, G. Wyszogrodzka, K. Młyniec and T. Librowski, Inflammopharmacology, 2017, 25, 11-24.
- 16 C. P. Larson, U. R. Saha and H. Nazrul, PLoS Med., 2009, 6, e1000175.
- 17 M. Porchia, M. Pellei, F. Del Bello and C. Santini, Molecules, 2020, 25, 5814.
- 18 C. I. Chukwuma, S. S. Mashele, K. C. Eze, G. R. Matowane, S. Md. Islam, S. L. Bonnet, A. E. M. Noreljaleel and L. M. Ramorobi, *Pharmacol. Res.*, 2020, **155**, 104744.
- 19 J. d'Angelo, G. Morgant, N. E. Ghermani, D. Desmaele, B. Fraisse, F. Bonhomme, E. Dichi, M. Sghaier, Y. Li,

- Y. Journaux and J. R. J. Sorenson, *Polyhedron*, 2008, 27, 537-546.
- 20 Q. Zhou, T. W. Hambley, B. J. Kennedy, P. A. Lay, P. Turner, B. Warwick, J. R. Biffin and H. L. Regtop, *Inorg. Chem.*, 2000, 39, 3742–3748.
- 21 H. Ali, S. Omar, M. Darawsheh and H. Fares, J. Coord. Chem., 2016, 69, 1110–1122.
- 22 C. Kakoulidou, S. Kalogiannis, P. Angaridis and G. Psomas, *Polyhedron*, 2019, **166**, 98–108.
- 23 M. Sumar Ristovic, A. Zianna, G. Psomas, A. Hatzidimitriou, E. Coutouli-Argyropoulou and M. Lalia-Kantouri, *Mater. Sci. Eng.*, C, 2016, 61, 579–590.
- 24 A. Zianna, G. Geromichalos, E. Psoma, S. Kalogiannis, A. G. Hatzidimitriou and G. Psomas, J. Inorg. Biochem., 2022, 229, 111727.
- 25 A. Zianna, G. Psomas, A. Hatzidimitriou, E. Coutouli-Argyropoulou and M. Lalia-Kantouri, *J. Inorg. Biochem.*, 2013, 127, 116–126.
- 26 A. Zianna, G. Psomas, A. Hatzidimitriou and M. Lalia-Kantouri, RSC Adv., 2015, 5, 37495–37511.
- 27 A. Zianna, G. Psomas, A. Hatzidimitriou and M. Lalia-Kantouri, *J. Inorg. Biochem.*, 2016, **163**, 131–142.
- 28 A. Zianna, G. D. Geromichalos, A. G. Hatzidimitriou, E. Coutouli-Argyropoulou, M. Lalia-Kantouri and G. Psomas, *J. Inorg. Biochem.*, 2019, **194**, 85–96.
- 29 Y. J. Han, L. Wang, Q.-B. Li and L. W. Xue, *Acta Chim. Slov.*, 2017, **64**, 179–185.
- 30 Q. Wu, Y. Tang, L. Xu, Y. Lei, T. Liu, F. Jiang, Q. Zi and Y. Qiao, *Z. Kristallogr. New Cryst. Struct.*, 2018, 233, 967–968.
- 31 J. Marmur, J. Mol. Biol., 1961, 3, 208-211.
- 32 M. F. Reichmann, S. A. Rice, C. A. Thomas and P. Doty, J. Am. Chem. Soc., 1954, 76, 3047–3053.
- 33 Bruker Analytical X-ray Systems, Inc. Apex2, Version 2 User Manual, M86-E01078, Madison, WI, 2006.
- 34 Siemens Industrial Automation, Inc., SADABS: Area– Detector Absorption Correction, Madison, WI, 1996.
- 35 L. Palatinus and G. Chapuis, *J. Appl. Crystallogr.*, 2007, **40**, 786–790.
- 36 P. W. Betteridge, J. R. Carruthers, R. I. Cooper, K. Prout and D. J. Watkin, *J. Appl. Crystallogr.*, 2003, **36**, 1487.
- 37 W. J. Geary, Coord. Chem. Rev., 1971, 7, 81-122.
- 38 K. Nakamoto, Infrared and Raman Spectra of Inorganic and Coordination Compounds, Part B: Applications in Coordination, Organometallic, and Bioinorganic Chemistry, Wiley, New Jersey, sixth Ed., 2009.
- 39 N. Raman and S. Sobha, *Spectrochim. Acta, Part A*, 2012, **93**, 250–259.
- 40 T. Topala, A. Bodoki, L. Oprean and R. Oprean, *Clujul Med.*, 2014, **87**, 215–219.

- 41 N. Shahabadi, S. M. Fili and S. Kashanian, *J. Coord. Chem.*, 2018, 71, 329–341.
- 42 R. C. Marchi, I. A. S. Campos, V. T. Santana and R. M. Carlos, *Coord. Chem. Rev.*, 2022, **451**, 2142752.
- 43 B. M. Zeglis, V. C. Pierre and J. K. Barton, *Chem. Commun.*, 2007, 4565–4576.
- 44 Q. Zhang, J. Liu, H. Chao, G. Xue and L. Ji, *J. Inorg. Biochem.*, 2001, **83**, 49–55.
- 45 G. Pratviel, J. Bernadou and B. Meunier, *Adv. Inorg. Chem.*, 1998, 45, 251–262.
- 46 A. M. Pyle, J. P. Rehmann, R. Meshoyrer, C. V. Kumar, N. J. Turro and J. K. Barton, *J. Am. Chem. Soc.*, 1989, 111, 3053–3063.
- 47 A. Wolfe, G. Shimer and T. Meehan, *Biochemistry*, 1987, 26, 6392–6396.
- 48 A. Dimitrakopoulou, C. Dendrinou-Samara, A. A. Pantazaki, M. Alexiou, E. Nordlander and D. P. Kessissoglou, *J. Inorg. Biochem.*, 2008, 102, 618–628.
- 49 J. L. Garcia-Gimenez, M. Gonzalez-Alvarez, M. Liu-Gonzalez, B. Macias, J. Borras and G. Alzuet, *J. Inorg. Biochem.*, 2009, **103**, 923–934.
- 50 J. R. Lakowicz, *Principles of Fluorescence Spectroscopy*, Plenum Press, NY, 3rd edn, 2006.
- 51 G. Zhao, H. Lin, S. Zhu, H. Sun and Y. Chen, *J. Inorg. Biochem.*, 1998, **70**, 219–226.
- 52 D. P. Heller and C. L. Greenstock, *Biophys. Chem.*, 1994, **50**, 305–312.
- 53 X. M. He and D. C. Carter, *Nature*, 1992, **358**, 209–215.
- 54 C. Tan, J. Liu, H. Li, W. Zheng, S. Shi, L. Chen and L. Ji, J. Inorg. Biochem., 2008, 102, 347–358.
- 55 L. Stella, A. L. Capodilupo and M. Bietti, *Chem. Commun.*, 2008, 4744–4746.
- 56 V. Rajendiran, R. Karthik, M. Palaniandavar, H. Stoeckli-Evans, V. S. Periasamy, M. A. Akbarsha, B. S. Srinag and H. Krishnamurthy, *Inorg. Chem.*, 2007, 46, 8208–8221.
- 57 O. H. Laitinen, V. P. Hytonen, H. R. Nordlund and M. S. Kulomaa, *Cell. Mol. Life Sci.*, 2006, **63**, 2992–3017.
- 58 R. Cini, G. Giorgi, A. Cinquantini, C. Rossi and M. Sabat, *Inorg. Chem.*, 1990, 29, 5197–5200.
- 59 C. Kontogiorgis and D. Hadjipavlou-Litina, *J. Enzyme Inhib. Med. Chem.*, 2003, **180**, 63–69.
- 60 G. K. Jayaprakasha, L. Rao and K. Sakariah, *Bioorg. Med. Chem.*, 2004, **12**, 5141–5146.
- 61 S. Dairi, M. Carbonneau, T. Galeano-Diaz, H. Remini, F. Dahmoune, O. Aoun, A. Belbahi, C. Lauret, J. Cristol and K. Madani, *Food Chem.*, 2017, 237, 297–304.
- 62 C. Kontogiorgis, M. Ntella, L. Mpompou, F. Karallaki, A. Papadopoulos, D. Hadjipavlou-Litina and D. Lazari, J. Enzyme Inhib. Med. Chem., 2016, 31, 154–159.